Catalysis Today 202 (2013) 191–196

Contents lists available at SciVerse ScienceDirect

Catalysis Today

journal homepage: www.elsevier.com/locate/cattod

Hydrogen oxidation on ordered intermetallic phases of platinum and tin – A combined experimental and theoretical study

E. Santos[a,b], L.M.C. Pinto[b,c], G. Soldano[b], A.F. Innocente[c], A.C.D. Ângelo[c], W. Schmickler[b,*]

[a] Faculdad de Matemática, Astronomía y Física, IFEG-CONICET Universidad Nacional de Córdoba, Córdoba, Argentina
[b] Institute of Theoretical Chemistry, Ulm University D-89069 Ulm, Germany
[c] Lab Eletrocatálise, Faculdade de Ciências Univ Estadual Paulista, UNESP, Bauru-SP, Brazil

ARTICLE INFO

Article history:
Received 5 December 2011
Received in revised form 1 June 2012
Accepted 19 July 2012
Available online 13 September 2012

Keywords:
Intermetallic
Theory of electrocatalysis
Density functional theory
Hydrogen oxidation

ABSTRACT

Hydrogen oxidation on the surfaces of the intermetallic compounds Pt_3Sn, PtSn and $PtSn_2$ has been studied by the rotating disc electrode technique. Pt_3Sn and PtSn were found to be good catalysts, about as good as Pt, while $PtSn_2$ was inactive over the investigated range of potentials. Underpotential deposition of hydrogen is observed only on Pt_3Sn. These results are explained by theoretical calculations based on a theory developed within our own group, and by density functional theory.

1. Introduction

Intermetallic phases of platinum and tin have long been considered as promising catalysts for several reactions. For example, they are good catalysts for ethanol oxidation, especially in alkaline solutions [1–3], and also for hydrogen oxidation[4,5]. For the latter reaction their main interest lies in the fact that they are CO-tolerant, so that they could be used in fuel cells that are fed hydrogen contaminated with CO [6,7], as it is obtained by catalytic reforming. While there are quite a few experimental studies of their electrochemical properties, the few theoretical studies that exist do not treat the hydrogen reaction [8–10].

We believe that the combination of experiment with theory is particularly valuable. Therefore we have embarked on a combined study of hydrogen oxidation on the three intermetallics Pt_3Sn, PtSn and $PtSn_2$ in order to explore and understand their catalytic properties. We shall show, that the two platinum richer compounds are good catalysts for this reaction, while $PtSn_2$ is not. These results are in line with calculations based on a theory of hydrogen electrocatalysis proposed by two of us (E.S. and W.S.) [11].

2. Experimental

The ordered intermetallic phases Pt_3Sn, PtSn and $PtSn_2$ were obtained by melting of the corresponding pure metals, Pt (Alpha Aesar, 99.9%) and Sn (Berzog, 99.9%) weighed in the stoichiometric proportions, in an electric-arc furnace under Argon atmosphere. These stoichiometric proportions were selected from the respective phase diagram that assures the ordered intermetallic phases [12] and aiming to observe the influence of the compositions on the surfaces properties towards the hydrogen oxidation reaction (HOR) mechanism. Each melt was homogenized and transferred to a thermal furnace to achieve the stability and homogeneity of the predicted phase. The samples were characterized by X-ray Diffraction (XRD) and Scanning Electronic Microscopy-Energy Dispersive X-ray Spectrometry (SEM-EDX) techniques to verify the identity of the materials and their stoichiometric compositions. All the samples were unequivocally characterized as the predicted phases. Further experimental details on the synthesis and characterization of the materials have been described in our previous papers [13,4].

Electrochemical experiments were made in a conventional two-compartment cell designed for the rotating disc electrode (RDE) technique with a reversible hydrogen electrode (RHE) as reference system, a high surface area platinum wire as counter electrode and 0.15M H_2SO_4 (Merck, AR) as electrolyte kept at room temperature ($25 \pm 1\,^{\circ}C$). The working electrode, of polished Pt or intermetallic RDE, was used to study the mechanism of the HOR. The experiments were carried out with a Pine Instruments Analytical Rotator system coupled to an EG&G PAR model 283 Galvanostat-Potentiostat controlled by M270 software. Prior to each experiments the solution was purged with bubbling N_2 (White Martins, 5.0) for 15 min to remove traces of O_2, and then saturated with H_2 (AGA, SS) for 5 min.

* Corresponding author. Tel.: +49 731 5031340.

0920-5861/$ – see front matter © 2012 Elsevier B.V. All rights reserved.
http://dx.doi.org/10.1016/j.cattod.2012.07.044

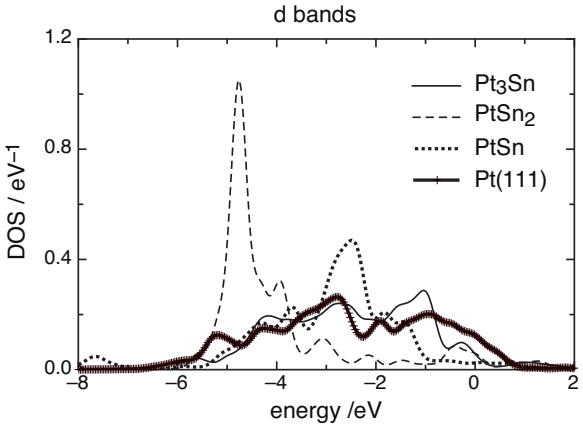

Fig. 1. DOS of the d bands for platinum atoms on the densest surface plane.

Also the working electrodes were submitted to a pretreatment of polishing with diamond paste.

Steady state measurements were performed by a chronoamperometric technique. Before each measurement, the electrode was kept at the equilibrium potential, where no current flows, and then stepped to the desired potential; the corresponding steady-state current was recorded after 10 s. During the data acquisition the electrode was rotated at 3500 rpm. A few other rotation speeds were also tested, and no significant difference was observed in the data collected. The electrode potential interval scanned was 0–30 mV, which is sufficient to obtain the exchange current densities, which are a good measure of the catalysis.

The details of the DFT calculations are given in the appendix.

3. Results and discussion

3.1. Electronic properties of the bimetallics

The experiments have been carried out on polycrystalline samples; we have performed calculations for surfaces with a low surface energy, which occur with the highest weight in polycrystalline samples. Hydrogen electrocatalysis is determined by the d band and its coupling to the hydrogen 1s orbital. Therefore we have calculated the structure of the platinum d band for the three intermetallics investigated and compared it to that of pure platinum. Fig. 1 shows the density of states (DOS) of the platinum atom on the densest surface planes. Remarkably, in the intermetallics the d band lies below the Fermi level, indicating that the platinum atoms have accepted electrons from tin, and the d band is filled. This is in line with the significant changes, compared to pure Pt, in the electronic density that have been observed in the intermetallics by XPS [13]. The d bands become narrower with increasing concentration of Sn, since the overlap between the d orbitals of the platinum atoms becomes smaller. Also, the d band center of $PtSn_2$ lies much lower than those of the other metals, where it lies roughly at the same position.

The work function of a few investigated surfaces are shown in Table 1; as expected, it increases with the density of Pt atoms on the surface. The corresponding surface structures are shown in Tables 2–5.

Table 1
Work functions of the investigated surfaces.

Surface	Work function/eV
Pt(1 1 1)	5.67
Pt_3Sn(1 1 1)	5.22
PtSn(1 1 $\bar{2}$0)	4.63
PtSn(0 0 0 1)	5.06
$PtSn_2$(1 0 0)	4.65

Table 2
Hydrogen adsorption distance d and adsorption free energy ΔG_{ad} on Pt_3Sn(1 1 1) at SHE.

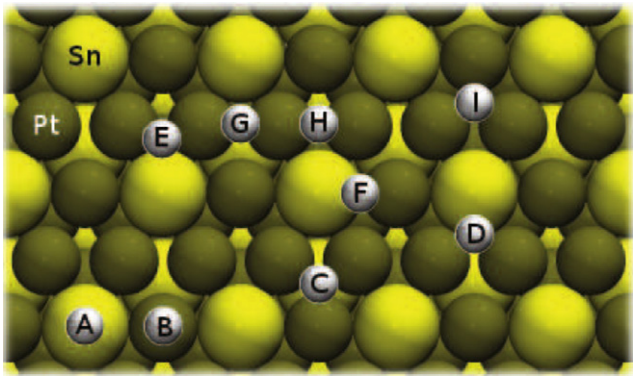

Label	Site	d/Å	ΔG_{ad}/eV
A	on top Sn	2.245	1.045
B	on top Pt	1.634	−0.209
C	hollow hcp Pt	0.913	−0.557
D	hollow fcc Pt_2–Sn	1.030	0.290
E	hollow hcp Pt_2–Sn	1.015	0.258
F	bridge Pt–Sn	1.258	0.680
G	bridge Pt–Pt over Sn	1.091	−0.397
H	bridge Pt–Pt over Pt	1.054	0.020
I	hollow fcc Pt	0.783	−0.216

3.2. Hydrogen adsorption

The intermediate of hydrogen oxidation is an adsorbed hydrogen atom. Its energy is one of the factors that determine the overall reaction rate: according to Sabatier's principle the optimum energy at the equilibrium potential is such that both reaction steps have vanishing reaction free energy [14–18]. We have therefore calculated the free energies ΔG_{ad} of adsorption of hydrogen at the standard hydrogen potential (SHE) for various sites on selected surfaces of the intermetallics. In general, we have focused on the surfaces with the lowest surface energies, because they predominate on polycrystalline metals. The energies have been obtained from DFT calculations, whose details are given in the appendix; they have been converted to free energies by adding 0.2 eV for the entropy contribution of the hydrogen gas [19,11].

Pt_3Sn is the intermetallic with the highest platinum content, and is expected to show a high affinity for hydrogen adsorption. Indeed, the (1 1 1) surface, which we have studied in detail, offers a multitude of adsorption sites, and several of them have negative adsorption free energies at SHE, implying that, just like on Pt, hydrogen adsorption sets in before hydrogen evolution – a phenomenon known as underpotential deposition (upd) of hydrogen. On the hollow hcp site (site C in Table 2) the adsorption energy is even more negative than on Pt(1 1 1). There are several sites with $\Delta G_{ad} \approx 0$, which are thus energetically suitable as intermediate states.

On PtSn we have found one site – the on top Pt site on PtSn(0 0 0 1), see Table 3 – with a negative adsorption free energy. However, the surface energy of this particular face, which is rich in Pt, has a value of 0.084 eV $Å^{-2}$ and is higher than that of PtSn(1 1 $\bar{2}$ 0) (0.059 eV $Å^{-2}$). Therefore, the (0 0 0 1) surface will not occur with a high density on a polycrystalline sample. Consequently, we expect little or no hydrogen upd on PtSn. On PtSn(1 1 $\bar{2}$ 0) the Pt–Pt bridge site has the most favorable adsorption energy near zero at SHE (see Table 4). In contrast, on $PtSn_2$(1 0 0) hydrogen adsorption at SHE is endergonic on all sites investigated – see Table 5.

Table 3
Hydrogen adsorption distance d and adsorption free energy ΔG_{ad} on PtSn(1 1 $\bar{2}$ 0) at SHE.

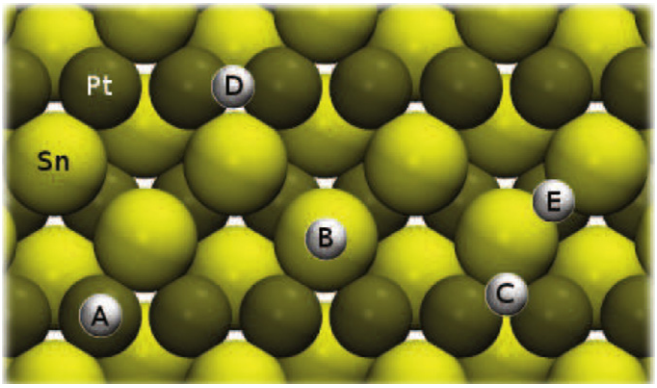

label	site	d/Å	ΔG_{ad}/eV
A	on top Pt	1.659	0.329
B	on top Sn	1.872	0.613
C	hollow Pt_2–Sn	1.141	0.737
D	bridge Pt–Pt	1.112	0.031
E	bridge Sn–Sn	1.079	0.623

In order to understand better the sizable differences in the hydrogen adsorption energies, we have plotted the DOS of the 1s orbital of the adsorbed hydrogen atom for the most strongly adsorbed species on Pt_3Sn(1 1 1) and on PtSn(1 1 $\bar{2}$ 0) (see Fig. 2). On the former surface the hydrogen DOS shows an unoccupied antibonding peak just above the Fermi level, which does not occur on PtSn(1 1 $\bar{2}$ 0). This peak is caused by the interaction with the d band, which on Pt_3Sn(1 1 1) lies higher than on PtSn(1 1 $\bar{2}$ 0). This empty antibonding peak shows that the d band participates in the bonding, and thus strengthens the adsorption bond. Obviously, these results are consistent with the d-band model of Hammer and Nørskov [20].

In summary, our calculations predict: strong hydrogen upd on Pt_3Sn, little or no upd on PtSn, and definitely none on $PtSn_2$. These expectations are borne out by the cyclic voltammograms shown in Fig. 3. Only Pt_3Sn shows a hydrogen upd region, which has, however, much less structure than that on polycrystalline Pt. The absence of structure could be due to the multitude of sites with different adsorption energies. Also, the interaction between adsorbed

Table 4
Hydrogen adsorption distance d and adsorption free energy ΔG_{ad} on PtSn(0 0 0 1) at SHE.

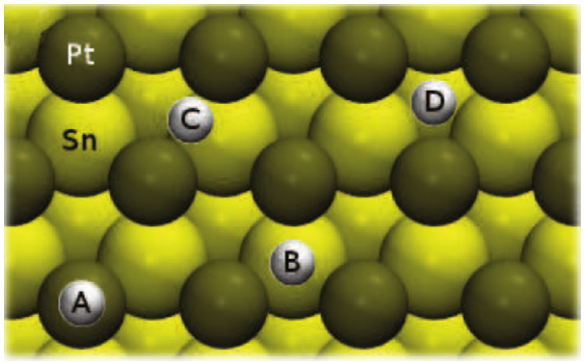

label	site	d/Å	ΔG_{ad}/eV
A	on top Pt	1.694	−0.380
B	hollow hcp	0.741	0.679
C	bridge Pt–Pt	0.527	0.276
D	hollow fcc	0.410	0.465

Table 5
Hydrogen adsorption distance d and adsorption free energy ΔG_{ad} on $PtSn_2$(1 0 0) at SHE.

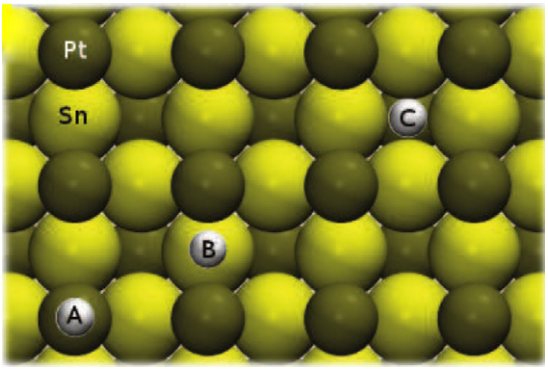

label	site	d/Å	ΔG_{ad}/eV
A	on top Pt	1.284	0.400
B	bridge Pt–Pt	0.260	0.915
C	hollow	−1.71	1.216

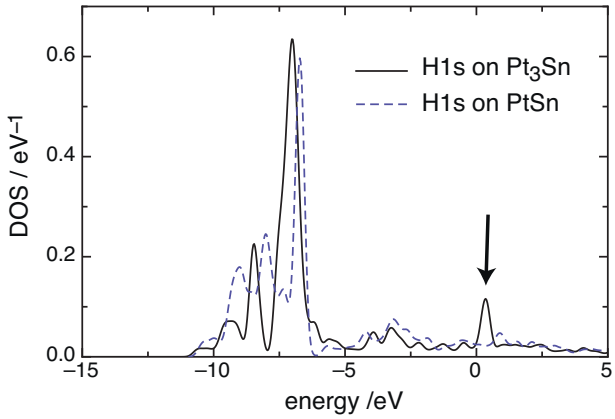

Fig. 2. DOS of the hydrogen atoms adsorbed at the most favorable sites on Pt_3Sn(1 1 1) (full line) and on PtSn(1 1 $\bar{2}$ 0) (dashed line); the arrow indicates the antibonding state on the former surface.

sulphate and hydrogen, which causes much of the structure on Pt, does probably not occur on Pt_3Sn because there are no Pt sites on which both sulphate and hydrogen could co-adsorb in a regular pattern. The intermetallics PtSn and $PtSn_2$ do not show hydrogen upd. Instead, they exhibit surface oxidation and reduction, with no extra current that could be attributed to hydrogen.

3.3. Hydrogen oxidation

A full account of the experiments will be published elsewhere, here we present the measured exchange current densities, which are a measure of the catalytic activity, and are directly relevant to this study. Table 6 gives the exchange current densities obtained on polycrystalline platinum and on the three intermetallic compounds investigated. The data on platinum are in good agreement

Table 6
Exchange current density j_0, at various electrode materials; all data were obtained in 0.15 M H_2SO_4 at room temperature (25 ± 1 °C).

electrode	j_0/mA cm^{-2}
Pt	1.1
Pt_3Sn	1.0
PtSn	1.5
$PtSn_2$	no activity

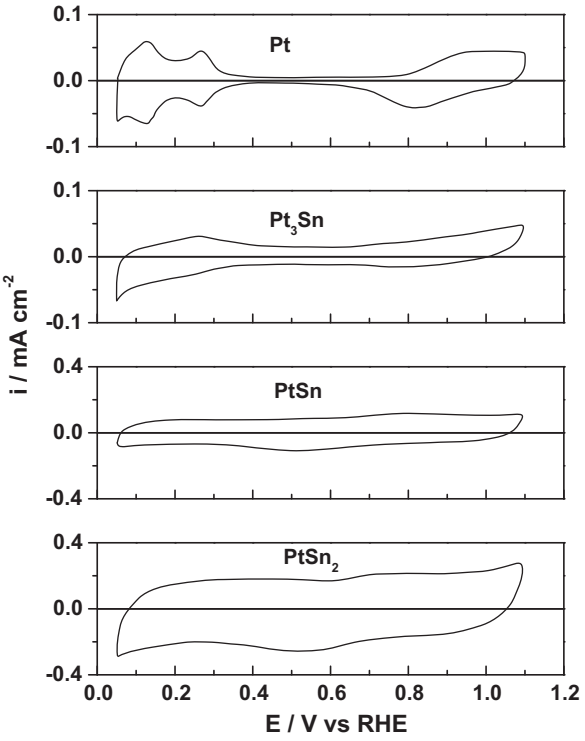

Fig. 3. Cyclic voltammograms of pure Pt and of the three bimetallics investigated in a 0.15 M solution of H_2SO_4; scan rate: 50 mV s^{-1}. The currents densities are given per geometric area.

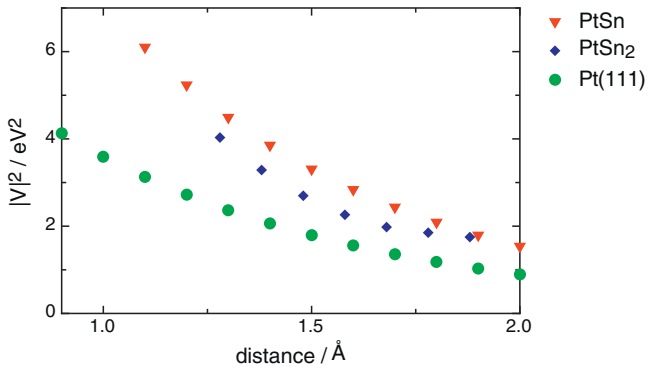

Fig. 4. Coupling $|V|^2$ between selected sites on PtSn and $PtSn_2$ as a function of distance. For comparison, Pt(1 1 1) is also shown.

with studies previously published in the literature [21,22] attesting the reliability of the data obtained in the present investigation. A value of $j_0 = 0.98$ mA cm^{-2} was calculated from the experiments of Markovich et al. [21], which matches the value obtained by us. The Pt_3Sn and PtSn surfaces showed a similar activity to Pt, while $PtSn_2$ was inactive over the investigated range of potentials. For the intermetallic compounds, the current densities are given per geometric area, since the real area is difficult to determine. However, for the present study the important point is that these compounds are about as active as platinum; therefore the uncertainty introduced by the surface area does not matter. All compounds were stable under working conditions. Even after a few hundred cycles there were no signs of metal dissolution, nor for surface segregation [4,5].

The fact that Pt_3Sn and PtSn are as active as Pt, while $PtSn_2$ shows no activity at all, is surprising, and requires some explanations. Two of us (E.S. and W.S.) [23,24] have developed a theory for hydrogen electrocatalysis which goes beyond DFT, and makes it possible to calculate free energy surfaces for the reaction. In order to make this paper self contained, we briefly summarize the main points of this theory in terms of the Volmer reaction: $H^+ + e^- \leftrightarrow H_{ad}$. The initial state is a strongly-solvated proton, whose 1s orbital lies above the Fermi level; the final state is an adsorbed, unsolvated hydrogen atom with one electron in the 1s state. According to the Marcus-Hush theory [25,26], the reaction occurs when a solvent fluctuation shifts the valence orbital of the proton to the Fermi level, where it gets filled, and the resulting hydrogen atom is adsorbed. Thus, the solvent plays an essential role, and in our theory its state is characterized by a solvent coordinate q familiar from Marcus theory. This has been normalized in such a way, that a solvent characterized by a coordinate q would be in equilibrium with a reactant of charge $-q$. The electronic interactions of the reactant with the metal electrode have been included by using elements from Anderson–Newns theory [27,28]. The combination of this theory with Marcus theory gives a complete description of the reaction, but it suffers from the fact that Anderson–Newns theory does not fully account for electronic many-body effects. Therefore, the model is combined with DFT in the following way: the electronic energy of the hydrogen atom, in various positions, is calculated by DFT; the electronic energy of the proton is zero. We interpolate between these two values with our theory, which in addition contains the solvation effects. This allows us to calculate free energy surfaces for the reaction, which for the Volmer reaction we may plot as a function of the distance of the reaction from the surface, and of the solvent coordinate q. In addition, the electronic coupling between hydrogen and the electrode is also obtained by DFT. In contrast to pure DFT, this theory includes the important solvent fluctuations and allows an explicit inclusion of the electrode potential.

While this theory allows quantitative calculations, its qualitative aspects can be summarized in three conditions which a good catalyst must fulfill: (1) a d band that lies near the Fermi level and that catalyzes the electron transfer as the orbital passes the Fermi level; (2) an adsorption energy $\Delta G_{ad} \approx 0$ at SHE (Sabatier's principle discussed above), and (3) a strong and long-ranged coupling with the 1s orbital of hydrogen – the long range is important because electron transfer occurs at a certain distance. In view of these conditions it is not surprising that Pt_3Sn with its high platinum content is a good catalyst, but for the other two bimetallics the matter is not so clear. We have therefore selected sites with favorable adsorption energies – the Pt–Pt bridge site on PtSn(1 1 $\bar{2}$ 0) and the on top Pt site on $PtSn_2$(1 0 0) – and calculated their interaction with the hydrogen 1s orbital as a function of the distance, using the procedure detailed in [11]. The resulting coupling constants $|V|^2$ are shown in Fig. 4. On both intermetallics the coupling is somewhat stronger than on pure platinum; we attribute this to the fact that on the bimetallics, in contrast to pure platinum, the d bands are filled, and that the platinum atoms bind to fewer platinum neighbours. Thus, the interaction with the hydrogen 1s orbital is strong on both surfaces, and is as long-ranged as on platinum.

Using the theory described above, we have calculated the free energy surfaces for the Volmer reaction, $H^+ + e^- \leftrightarrow H_{ad}$ at the potential of the standard hydrogen electrode both for the most favorable sites on both on PtSn(1 1 $\bar{2}$ 0) and on $PtSn_2$(1 0 0) (see Fig. 5). Both plots show the free energy as a function of the distance and of the solvent coordinate q. The proton appears at $q = -1$ and far from the surface; the adsorbed hydrogen atom is uncharged, so it appears at $q = 0$ and right on the surface. The optimum path between these two states passes over a saddle point, whose height determines the energy of activation.

In the case of PtSn(1 1 $\bar{2}$ 0) the strong coupling between the reactants to some extent compensates for the position of the d band, which is less favorable than on Pt(1 1 1). The activation energy of about 0.44 eV is quite favorable. For the Tafel reaction $H_2 \rightarrow 2H_{ad}$ we obtained an activation energy of about 0.32 eV. Within the

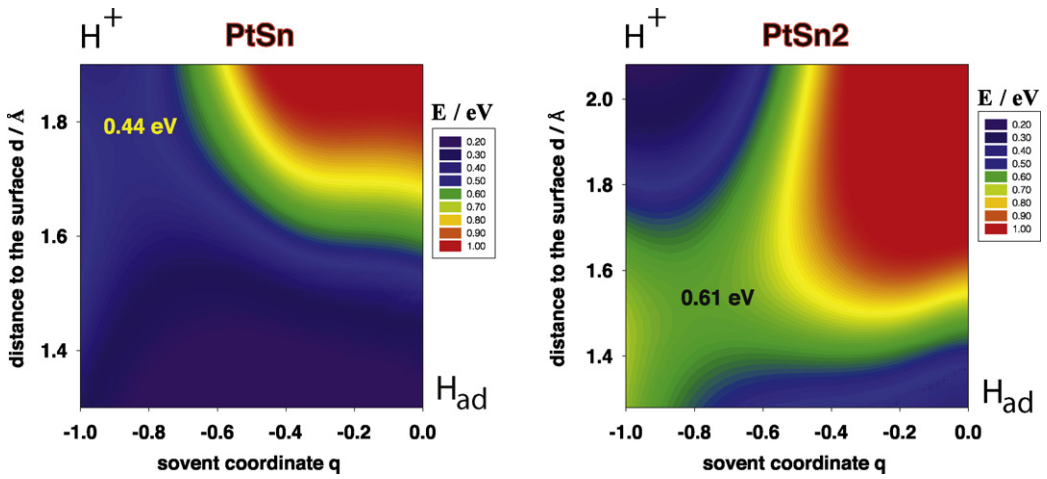

Fig. 5. Free energy surfaces for the Volmer reaction on PtSn and $PtSn_2$ at SHE.

error of our calculations both steps have about the same activation energy; however, with increasing overpotential the Volmer reaction should become faster, while the Tafel reaction, being a purely chemical step, should be independent of potential. A comparison with Pt(1 1 1) is difficult, since on this metal there are two different adsorbed species, the strongly adsorbed (underpotential deposited) H_s, and the weakly adsorbed H_w. Both species compete with each other, and affect also the activation energies both for the Volmer and for the Tafel step; the theoretical details are discussed in [24], a kinetic analysis is given in [29]. Near SHE the Tafel reaction determines the overall rate, and according to our calculations its activation energy is of the order of 0.3–0.5 eV, its exact value depending on the coverage with H_s, which changes with the electrode potential [24]. Similarly, the rate of the Volmer reaction on Pt(1 1 1) also depends on the coverage with the strongly adsorbed species H_s, and for full coverage we obtained an activation barrier of about 0.3 eV. Overall, the theoretical data are in line with the experimental observation that on Pt(1 1 1) and PtSn hydrogen oxidation proceeds with about the same rate.

On $PtSn_2$ the most favorable site has an adsorption free energy of about 0.4 eV; for the Volmer step we have obtained an activation energy of about 0.61 eV, substantially higher than on PtSn. Thus, according to our estimate this step is slower by a factor of about 10^{-3} than on PtSn, which explains why no current was observed in the limited range of potential investigated. For the Tafel reaction $H_2 \rightarrow 2H_{ad}$ we obtained an activation energy of about 0.65 eV, again much larger than on PtSn, and of the same order of magnitude as for the Volmer reaction at SHE. The most favorable site for the breaking of the hydrogen bond was above a platinum atom.

4. Conclusion

In this work, we have investigated hydrogen oxidation on the three bimetallic compounds Pt_3Sn, PtSn, and $PtSn_2$ both experimentally and theoretically. Experimentally, both Pt_3Sn and PtSn showed about the same activity as pure Pt, while $PtSn_2$ was inactive in the potential range investigated. However, only Pt_3Sn exhibits underpotential deposition of hydrogen. The theoretical calculations showed that the d band of the surface platinum atoms is filled in all three compounds, indicating that electrons have been transferred from the less electronegative tin. The free energies of adsorption of hydrogen are in accord with the experimental findings concerning the occurrence of upd. On Pt_3Sn there are a variety of sites on which at SHE hydrogen adsorption is exergonic. On PtSn we found only one such site, and on a surface with high energy, and on $PtSn_2$ hydrogen adsorption at SHE is endergonic on all sites. That the platinum-rich Pt_3Sn is a good catalyst is no great surprise. Less expected are the findings that both theory and experiment indicate, that PtSn is about as good. According to our calculations this is due to two effects: the absence of strongly adsorbed (upd) hydrogen, which inhibits the reaction [24], and the large coupling constant with the hydrogen 1s orbital.

The overall agreement between experimental and theoretical results is quite satisfying, particularly since both parts proceeded independently. The theoretical results had been obtained in Ulm before the experimental data from Bauru were available, and were thus a prediction largely fulfilled by experiment.

Details of DFT calculations

All calculations were performed using the dacapo code [30]. This utilizes an iterative scheme to solve the Kohn–Sham equations of density-functional theory self-consistently. A plane-wave basis set is used to expand the electronic wave functions, and the inner electrons were represented by ultrasoft pseudopotentials [31], which allow the use of a low-energy cutoff for the plane-wave basis set. An energy cutoff of 400 eV, dictated by the pseudopotential of each metal, was used in all calculations. The electron–electron exchange and correlation interactions are treated with the generalized gradient approximation in the version of Perdew et al [32]. The Brillouin-zone integration was performed using a $8 \times 8 \times 1$ k-point Monkhorst-Pack grid [33] corresponding to the 1×1 surface unit cell. Spin polarization was considered for the hydrogen atoms at larger distances; typically, spin polarization on these atoms occurs at distances larger than 2.4 Å. In all cases considered, electron transfer to the proton takes place at shorter distances, so the spin polarization of hydrogen has no effect. A dipole correction was used to avoid slab–slab interactions [34]. The DFT calculations give the adsorption energies; these were converted to free energies by adding an entropy contribution of 0.2 eV [19].

For all the systems, the two bottom layers were fixed at the nearest-neighbor distance corresponding to bulk, and all the other layers were allowed to relax. The convergence criterion was achieved when the total forces were less than 0.02 eV/Å. Activation barriers for the Tafel reaction were obtained from the nudged elastic band method [35].

Acknowledgments

Financial supports by the Deutsche Forschungsgemeinschaft (Schm 344/34-1,2, Sa 1770/1-1,2, and FOR 1376), and by the European Union under ELCAT are gratefully acknowledged. E. S.,

and W.S. thank CONICET for continued support. A generous grant of computing time from the Baden-Württemberg grid is gratefully acknowledged. L.M.C.P. thanks the DAAD for a stipend. A.F.I., L.M.C.P and A.C.D.A are grateful to the following Brazilian authorities: Fundação de Amparo a Pesquisa do Estado de São Paulo (FAPESP), Conselho Nacional de Desenvolvimento Científico e Tecnológico (CNPq) and Financiadora de Estudos e Projetos (FINEP).

References

[1] M. Zhu, G. Sun, Q. Xin, Electrochimica Acta 54 (2009) 1511–1518.
[2] L. Jiang, G. Sun, Z. Zhou, W. Zhou, Q. Xin, Catalysis Today 93–95 (2004) 665–670.
[3] E.R. Gonzalez, E.A. Ticianelli, E. Antolini, in: E. Santos, W. Schmickler (Eds.), Catalysis in Electrochemistry, John Wiley & Sons, Inc., Hoboken, 2011, pp. 453–485.
[4] A.F. Innocente, A.C.D. Ângelo, Journal of Power Sources 162 (2006) 151–159.
[5] A.F. Innocente, A.C.D. Ângelo, Journal of Power Sources 175 (2008) 779–783.
[6] Z. Liu, G.S. Jackson, B.W. Eichhorn, Angewandte Chemie International Edition 49 (2010) 3173–3176.
[7] E. Casado-Rivera, D.J. Volpe, L. Alden, C. Lind, C. Downie, T. Vazquez-Alvarez, A.C.D. Ângelo, F.J. DiSalvo, H.D. Abruña, Journal of the American Chemical Society 126 (2004) 4043–4049.
[8] R.M. Watwe, R.D. Cortright, M. Mavrikakis, J.K. Nørskov, J.A. Dumesic, Journal of Chemical Physics 114 (2001) 4663–4668.
[9] R. Alcala, J.W. Shabaker, G.W. Huber, M.A. Sanchez-Castillo, J.A. Dumesic, Journal of Physical Chemistry B 109 (2005) 2074–2085.
[10] Z.-F. Xu, Y. Wang, Journal of Physical Chemistry C 115 (2011) 20565–20571.
[11] E. Santos, A. Lundin, K. Pötting, P. Quaino, W. Schmickler, Physical Review B 79 (2009) 235436-1–235436-10.
[12] T.B. Massalski, Binary Alloy Phase Diagrams, vol. 03, second ed., ASM International, Ohio, 1990.
[13] L.M.C. Pinto, E.R. Silva, R. Caram-Jr, G. Tremiliosi-Filho, A.C.D. Ângelo, Intermetallics 16 (2008) 246–254.
[14] P. Sabatier, La catalyse en chimie organique, C. Béranger, Paris, 1920.
[15] H. Gerischer, Zeitschrift fur Physikalische Chemie 8 (1956) 137–153.
[16] R. Parsons, Transactions of the Faraday Society 54 (1958) 1053–1063.
[17] S. Trasatti, Journal of Electroanalytical Chemistry 39 (1972) 163–184.
[18] J.K. Nørskov, T. Bligaard, A. Logadottir, J.R. Kitchin, J.G. Chen, S. Pandelov, U. Stimming, Journal of The Electrochemical Society 152 (2005) J23–J26.; W. Schmickler, S. Trasatti, Journal of The Electrochemical Society 153 (2006) L31–L32.
[19] G.S. Karlberg, T.F. Jaramillo, E. Skúlason, J. Rossmeisl, T. Bligaard, J.K. Nørskov, Physical Review Letters 99 (2007) 126101-1–126101-4.
[20] B. Hammer, J.K. Nørskov, Advances in Catalysis 45 (2000) 71–129.
[21] N.M. Markovic, B.N. Grgur, P.N. Ross, Journal of Physical Chemistry B 101 (1997) 5405–5413.
[22] R.M.Q. Mello, E.A. Ticianelli, Electrochimica Acta 42 (1997) 1031–1039.
[23] E. Santos, W. Schmickler, Angewandte Chemie International Edition 46 (2007) 8262–8265.
[24] E. Santos, P. Hindelang, P. Quaino, E.N. Schulz, G. Soldano, W. Schmickler, ChemPhysChem 12 (2011) 2274–2279.
[25] R.A. Marcus, Journal of Chemical Physics 24 (1956) 966–978.
[26] N.S. Hush, Journal of Chemical Physics 28 (1958) 962–972.
[27] P.W. Anderson, Physical Review 124 (1961) 41–53.
[28] D.M. Newns, Physical Review 178 (1969) 1123–1135.
[29] P.M. Quaino, M.R. Gennero de Chialvo, A.C. Chialvo, Electrochimica Acta 52 (2007) 7396–7403.
[30] B. Hammer, L.B. Hansen, J.K. Nørskov, Physical Review B 59 (1999) 7413–7421, http://www.fysik.dtu.dk/campos.
[31] D. Vanderbilt, Physical Review B 41 (1990) 7892–7895.
[32] J.P. Perdew, K. Burke, M. Ernzerhof, Physical Review Letters 77 (1996) 3865–3868.
[33] H.J. Monkhorst, J.D. Pack, Physical Review B 13 (1976) 5188–5192.
[34] L. Bengtsson, Physical Review B 59 (1999) 12301–12304.
[35] G. Henkelman, B.P. Uberuaga, H. Jónsson, Journal of Chemical Physics 113 (2000) 9901–9904.; G. Henkelman, H. Jónsson, Journal of Chemical Physics 113 (2000) 9978–9985.